Microelectronic Engineering 88 (2011) 775–778

Contents lists available at ScienceDirect

Microelectronic Engineering

journal homepage: www.elsevier.com/locate/mee

Optimal design for micro-thermoelectric generators using finite element analysis

Bongkyun Jang, Seungwoo Han *, Jeong-Yup Kim

Department of Nano Mechanics, Korea Institute of Machiney & Materials, 171 Jang-dong, Yuseong-gu, Daejeon 305-343, Republic of Korea

ARTICLE INFO

Article history:
Available online 3 July 2010

Keywords:
Micro-thermoelectric generator
Finite element analysis
Seebeck effect
Peltier effect

ABSTRACT

To fabricate micro-thermoelectric generators (μTEGs), one must design the optimal structure of the μTEGs and achieve thermoelectric thin films with excellent properties. This study investigated the role of the dimensions of μTEGs, including the length of the thermoelements, thickness of the substrates, and cross-sectional area of the thermoelements. To evaluate the power generated by μTEGs and their efficiency, three-dimensional models of μTEGs were subjected to finite element analysis. Three-dimensional models are more accurate than one-dimensional models, since the directions of the heat flux and electrical current are not parallel in μTEGs. The governing equations were derived from the Seebeck effect and Peltier effect, which show thermoelectric energy conversion. In the simulation, the substrate, n-type material, and p-type material were assumed to be silicon, Bi_2Te_3, and Sb_2Te_3, respectively. We calculated the thermoelectric power generated by the μTEGs and their thermoelectric energy conversion efficiency. These two evaluation indices represent the performance of μTEGs. The thermoelectric simulation produced design guidelines for high-performance μTEGs.

1. Introduction

For the sustainable development of humankind and to stop climate change as outlined in the Kyoto Protocol, the use of conventional energy sources such as fossil fuels will have to be limited in the very near future. New alternative sources of energy such as wind, hydropower, and solar energy are important research topics in physics, chemistry, biology, and mechanics. As one such alternative, thermoelectric energy has many favorable characteristics: light weight, small scale, and low manufacturing cost [1]. Given these advantages, thermoelectric modules have numerous applications, such as in the energy source for autonomous microsystems, harvesting energy from the waste heat from high-performance microprocessors, body-powered wearable and pocket devices, and semipermanent power for implanted medical devices [2–5].

Thermoelectric effects involve the reversible conversion of energy from thermal energy to electrical energy. The Seebeck effect refers to forward energy conversion and the Peltier effect is reverse conversion. These effects, which were discovered about 200 years ago, have not been used in power generator due to the low energy conversion efficiency [1]. However, many researchers have studied thermoelectric power generation since the possibility of enhancing the thermoelectric conversion efficiency using nanotechnology was reported [6,7].

To fabricate high-performance micro-thermoelectric generators (μTEGs), thermoelectric materials deposited using microelectromechanical systems (MEMS) processes in the form of thin films should have excellent thermoelectric properties, and a great deal of active research is now examining high-performance materials [8,9]. In addition to high-quality thermoelectric materials, the optimal design of an integrated module that includes thermoelectric materials, electrodes, and substrates is indispensable to achieve high-performance μTEGs. Some researchers have already studied the geometric dependence of thermoelectric modules using one-dimensional models [10–13]. However, these studies cannot explain the effects of various geometric shapes. Moreover, an accurate analysis is impossible when the directions of the heat flux and electrical current are not parallel in the thermoelements of μTEGs made from thin thermoelectric materials compared to the cross-sectional area. In this study, we investigated the optimal structure of high-performance μTEGs using the finite element method with three-dimensional models.

2. Formulation

2.1. Geometric configuration

We considered a conventional thermoelectric unit composed of a single p–n pair. Fig. 1 shows the π-shaped thermoelectric unit in which the p- and n-type thermoelements are connected in parallel thermally and in series electrically. The electrodes of the p- and n-type thermoelements are connected electrically. In addition, the upper and lower substrates play a role in thermal conduction from heat sources and cooling parts to the electrodes linking the thermoelements. They also function as an electrical insulation layer

* Corresponding author.
E-mail address: swhan@kimm.re.kr (S. Han).

0167-9317/$ - see front matter © 2010 Elsevier B.V. All rights reserved.
doi:10.1016/j.mee.2010.06.025

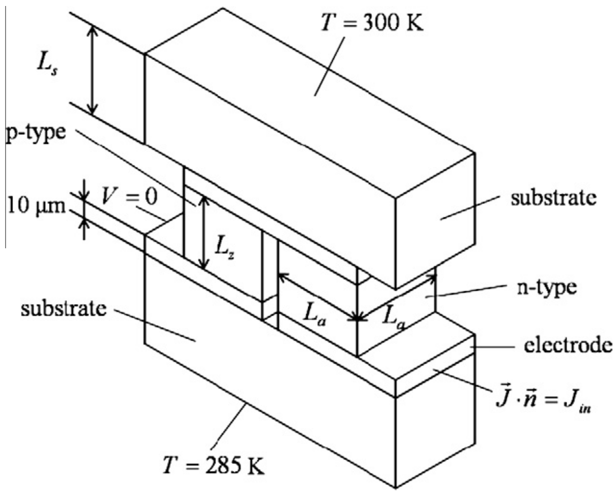

Fig. 1. Geometry of the micro-thermoelectric generation unit analyzed in this study.

between the outer heat source and cooling parts. We assume that the μTEGs are constructed from such thermoelectric units joined in series.

2.2. Governing equations

From the finite element analysis, we obtain steady-state solutions for the governing equations explained below. The governing equations express the thermal, electrical, and thermoelectric effects in the thermoelectric materials.

When temperature gradient ∇T is given, the electrical field $\vec{E}$ generated in the thermoelectric material is given by

$$\vec{E} = \alpha \nabla T - \rho \vec{J}, \tag{1}$$

from the Seebeck effect and Ohm's law. Here, α, ρ, and $\vec{J}$ denote the Seebeck coefficient, resistivity, and current density, respectively. The Peltier effect, which explains the heat flux $\vec{q}$ in the thermoelements, is expressed by

$$\vec{q} = \alpha T \vec{J} + \kappa \nabla T. \tag{2}$$

Here, the second term explains the thermal conduction with thermal conductivity κ. Eqs. (1) and (2) are partial differential equations that explain the thermoelectric effects in thermoelectric materials

$$\nabla \cdot \vec{q} = \vec{J} \cdot \vec{E}, \tag{3}$$

$$\nabla \cdot \vec{J} = 0, \tag{4}$$

$$\vec{E} = -\nabla V, \tag{5}$$

express the energy conservation law, continuity of current, and definition of the electrical potential V, respectively. Since we have five equations and five unknown variables, we can obtain the solution by solving these simultaneous partial differential equations with the finite element method.

Note that Eqs. (1) and (2) show Ohm's law and Fourier's law when $\alpha = 0$. In the electrodes, since the governing equations consist only of electrical and thermal conduction equations, Eqs. (1) and (2) are used in the analysis. Consequently, we can simply calculate the temperature distribution in the substrates using Eq. (2).

2.3. Simulation

We assumed the use of p- and n-type materials, such as Sb_2Te_3 and Bi_2Te_3, which have excellent thermoelectric properties at room temperature. The substrates and electrodes are silicon and copper, respectively, which are widely used materials in the MEMS process. The properties of these materials are shown in Table 1 [13].

Table 1
Properties of the materials used in the finite element analysis.

Materials	Thermal conductivity (κ)	Electrical conductivity (ρ)	Seebeck coefficient (α)
n-Type thermoelement (Bi_2Te_3)	1.6 W/m K	7.69×10^4 S/m	-2.28×10^{-4} V/K
p-Type thermoelement (Sb_2Te_3)	2.1 W/m K	9.62×10^4 S/m	1.71×10^{-4} V/K
Electrode (Cu)	350 W/m K	5.90×10^8 S/m	
Substrate (Si)	130 W/m K		

The boundary conditions are described in Fig. 1. The current flows through one side in an electrode, and the electrical potential is zero at the surface of the counter-side electrode. The temperatures at the top of the upper substrate and bottom of the lower substrate are 300 K and 285 K, respectively. For application as harvesters of wasted heat for wearable and pocket electronic devices, we performed the analysis with a relatively small difference in temperature [4]. The other boundaries are assumed to be adiabatic boundary conditions.

For a given electrical current flow into the unit, we calculated the electrical potential, temperature distribution, and heat flux. Then, the efficiency η of this unit is determined as

$$\eta = P/Q_{\text{in}}, \tag{6}$$

where P is the power generated in the unit and Q_{in} is the amount of heat flux through the hot side surface of the unit.

3. Results and discussion

First, we investigated the effect of the substrate, as shown in Figs. 2 and 3. As the thickness of the substrate increases, the thermal loss in the substrate becomes larger than that in the thermoelements. For this reason, the maximum difference in temperature and the maximum electrical potential of the unit are small when the substrates are thick. Therefore, the generated power decreases as the substrate gets thicker. Although the heat flux through the hot side surface also decreases in thick substrates, it

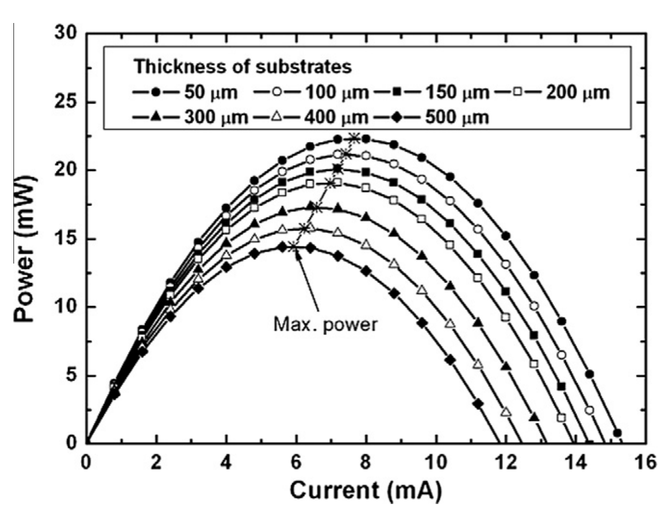

Fig. 2. Maximum power generated in thermoelectric units with various substrate thicknesses.

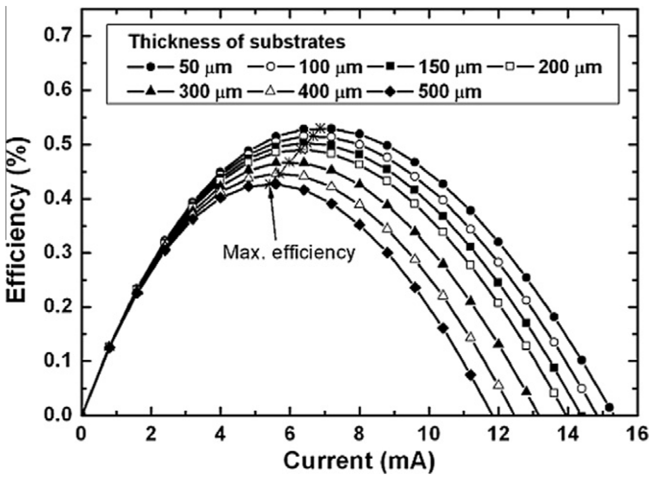

Fig. 3. Maximum efficiency obtained in thermoelectric units with various substrate thicknesses.

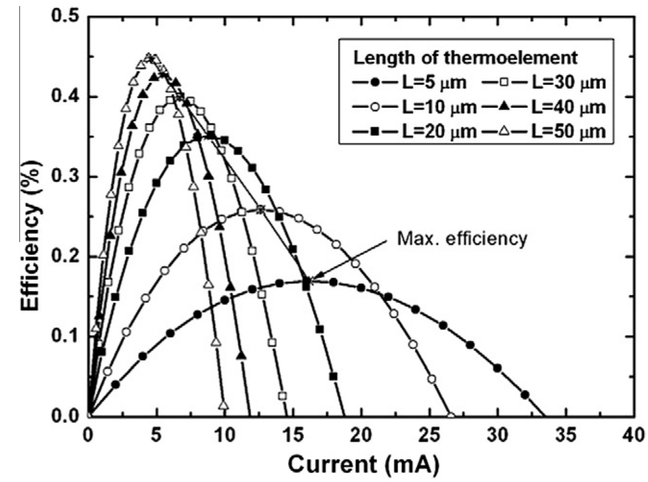

Fig. 5. Maximum efficiency obtained in thermoelectric units with thermoelements of various lengths.

is small compared to the reduction in the power generated by thick substrates. Hence, a unit with thick substrates has low efficiency.

To determine the geometric effects of the thermoelements, the dependences of the power and efficiency on the length of the thermoelements are shown in Figs. 4 and 5, respectively. Generally, power generated in the unit increases when the thermoelements are small due to the decrease in the electrical resistance. However, for short thermoelements, the difference in temperature between the upper and lower sides of the thermoelements decreases. For this reason, the length of the thermoelements is optimized to give the highest power. The efficiency tends to increase with the length of the thermoelements due to the dominant effect of the heat flux decrement.

Finally, we investigated the characteristics of a unit with thermoelements having various cross-sectional areas. The open circuit voltages, which are directly related to the maximum difference in temperature from Eq. (1), are large for units with small cross-sectional areas. However, the short circuit current is small, since the electrical resistance is large when the cross-sectional area of the thermoelements is small. Consequently, a large power output is obtained in a unit with thermoelements having large cross-sectional areas, as shown in Fig. 6. However, the efficiency decreases as illustrated in Fig. 7, when the cross-sectional area is

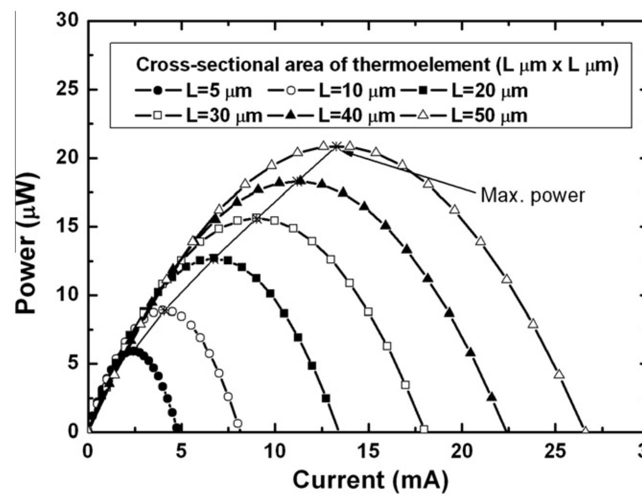

Fig. 6. Maximum power generated in thermoelectric units with thermoelements of various cross-sectional areas ($L \times L$ μm^2).

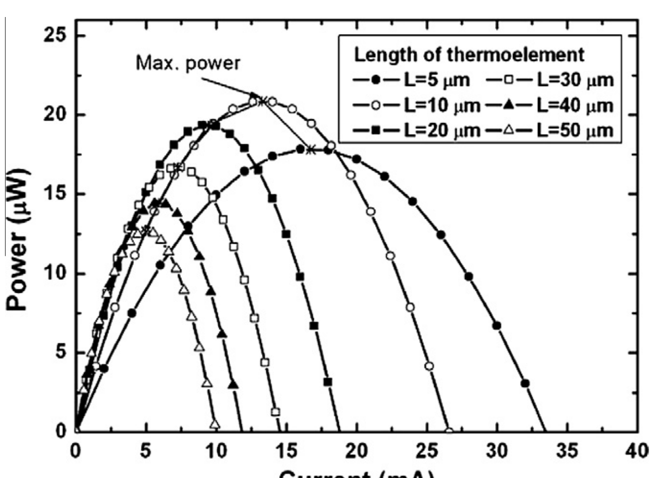

Fig. 4. Maximum power generated in the thermoelectric units with thermoelements of various lengths.

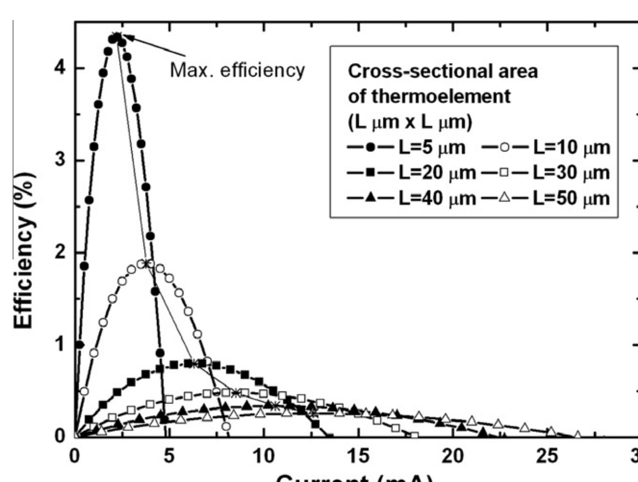

Fig. 7. Maximum efficiency obtained in thermoelectric units with thermoelements of various cross-sectional areas ($L \times L$ μm^2).

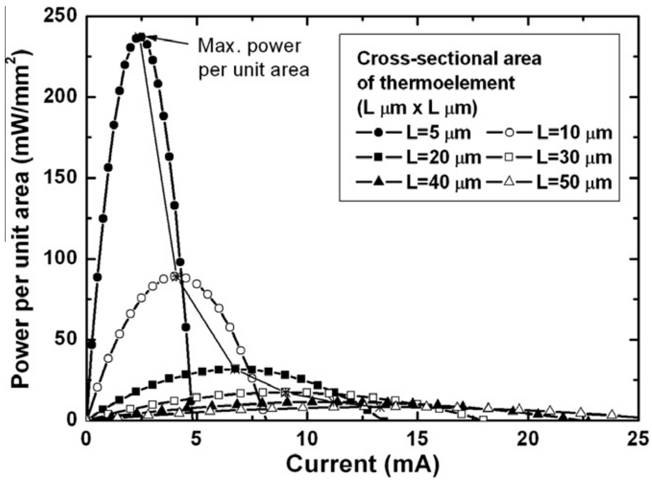

Fig. 8. Maximum power per unit area obtained in thermoelectric units with thermoelements of various cross-sectional areas ($L \times L$ μm^2).

large because the heat flux through the hot side is proportional to the cross-sectional area of the thermoelements. For the same reason, the power generated per unit area is small in a unit with a small cross-sectional area, as shown in Fig. 8. In contrast, the dependence of the power output per unit area is similar to that of the generated power on the substrate thickness and thermoelement length for the same unit area. The method used to evaluate the performance of μTEGs can be summarized using the generated power, power output per unit area, and efficiency. The efficiency given by Eq. (6) is the ideal parameter. However, measuring the efficiency of a thermoelectric module in practice is difficult due to the difficulty in measuring the heat flux. For this reason, μTEG manufacturers provide the generated power or power output per unit area in their data sheets. To develop μTEGs considering the usage and heat source, estimating the efficiency from an analysis of the module is essential.

4. Conclusions

The dependence of thermoelectric performance on the substrate thickness and the length and cross-sectional area of the thermoelements was investigated using finite element analysis with a three-dimensional model. As the substrate gets thicker, the thermoelectric performance deteriorates due to thermal loss from the substrate. The thermoelements have an optimal length with the highest power. High efficiency is obtained when the length of the thermoelements is large. The power generated declines with the cross-sectional area of the thermoelements, while the efficiency shows the opposite trend. The exact prediction of the efficiency using the analysis helps the engineer evaluate the thermoelectric module. To design high-performance μTEGs, the design parameters should be optimized by analyzing a three-dimensional model.

Acknowledgment

This study was supported by the R&D program for Energy and Resource Technology funded by the Ministry of Knowledge Economy.

References

[1] F.J. DiSalvo, Science 285 (1999) 703–706.
[2] Y. Yang, X.J. Wei, J. Liu, Journal of Physics D: Applied Physics 40 (2007) 5790–5800.
[3] K. Yazawa, G.L. Solbrekken, A. Bar-Cohen, IEEE Transactions on Advanced Packaging 28 (2005) 231–239.
[4] V. Leonov, R.J.M. Vullers, Journal of Electronic Materials 38 (2009) 1491–1498.
[5] S.M. Yang, T. Lee, M. Cong, Sensors and Actuators A: Physical 157 (2010) 258–266.
[6] L.D. Hicks, M.S. Dresselhaus, Physics Review B 47 (1993) 16631–16634.
[7] L.D. Hicks, M.S. Dresselhaus, Physics Review B 47 (1993) 12727–12731.
[8] R. Venkatasubramanian, E. Siivola, T. Colpitts, B. O'Quinn, Nature 451 (2001) 597–602.
[9] J.-S. Rhyee, K.H. Lee, S.M. Lee, E. Cho, S.I. Kim, E. Lee, Y.S. Kwon, J.H. Shim, G. Kotliar, Nature 459 (2009) 965–968.
[10] D.M. Rowe, G. Min, Journal of Power Sources 73 (1998) 193–198.
[11] G. Min, D.M. Rowe, Solid-State Electronics 43 (1999) 923–929.
[12] W. Glatz, S. Muntwyler, C. Hierold, Sensors and Actuators A 132 (2006) 337–345.
[13] L.W. Da Silva, M. Kaviany, International Journal of Heat Mass Transfer 47 (2004) 2417–2435.